J Mater Sci (2007) 42:5924–5935
DOI 10.1007/s10853-007-1773-9

Influence of microstructure on corrosion behavior of Ti–5%Ta–1.8%Nb alloy

R. Mythili · A. Ravi Shankar · S. Saroja · V. R. Raju · M. Vijayalakshmi · R. K. Dayal · V. S. Raghunathan · R. Balasubramaniam

Received: 17 March 2006 / Accepted: 8 December 2006 / Published online: 16 May 2007

Abstract This paper presents the results of a study on the influence of microstructure on the corrosion behavior of a α–β Ti–5%Ta–1.8%Nb alloy—a candidate material for use in high concentrations of boiling nitric acid. The ''as cast'' alloy had a lamellar structure and showed a corrosion rate of about 1.5 mpy. Thermo-mechanical processing of the cast alloy resulted in a structure of predominantly of equiaxed α with random distribution of fine β particles. This ''reference'' structure was further modified employing different heat treatments similar to that for commercial titanium alloys such as mill annealing, solution treatment and aging or over aging treatments. Corrosion rates evaluated in boiling nitric acid in the liquid, vapor and condensate phases, showed low values ~1 mpy. Of these, the lowest corrosion rate (~0.03 mpy) was exhibited by the structure with minimum amount of β phase, distributed in an equiaxed α matrix. This structure was obtained by aging of the solution treated ''reference'' alloy. Hence, solution treatment high in the $\alpha + \beta$ phase field followed by aging at a temperature low in the $\alpha + \beta$ phase field has been identified as the optimum treatment to obtain a microstructure with superior corrosion resistance.

R. Mythili · A. Ravi Shankar · S. Saroja (✉) · V. R. Raju · M. Vijayalakshmi · R. K. Dayal · V. S. Raghunathan
Metallurgy and Materials Group, Indira Gandhi Centre for Atomic Research, Kalpakkam 603 102, India
e-mail: saroja@igcar.gov.in

R. Balasubramaniam
Department of Materials and Metallurgical Engineering, Indian Institute of Technology, Kanpur 208 016, India

Introduction

Reprocessing of spent fuel from fast breeder reactors requires its dissolution in boiling nitric acid in a highly oxidizing condition, containing ions such as Cr^{6+}, Ag^{2+}, Ce^{4+}, $Cr_2O_7^{2-}$, and Fe^{3+}. Corrosion studies of candidate materials in boiling nitric acid with or without Uranium indicated good corrosion resistance of materials like Zircalloy-2, Ti–5%Ta and stainless steel grades like Uranus-16 and Uranus-65. Corrosion resistance of zirconium, titanium and its alloys was found to be good even in the presence of fission products with high redox potential [1, 2]. Commercial 304L grade of steel has shown severe intergranular and general attack in these media [1]. Zirconium has a high susceptibility to transgranular stress corrosion cracking (TGSCC) even in low concentrations of nitric acid, which is attributed to its anisotropy as a result of HCP structure. The susceptibility of Zirconium to cracking was also observed [3] in corrosion fatigue tests. Additionally, Zirconium weldments show a higher sensitivity to stress corrosion cracking (SCC) [3] in the heat-affected zone.

Titanium shows excellent corrosion resistance as a result of a continuous, stable, highly adherent, and protective oxide film. The nature, composition, and thickness of the protective surface oxide that forms on titanium alloys depend on environmental conditions. In most aqueous environments, the oxide is typically TiO_2, Ti_2O_3, or TiO [4]. The oxidation potential of boiling HNO_3 is high to form TiO_2 (rutile) though it is possible to form chemically unstable Ti_2O_3 [3]. Titanium has excellent corrosion resistance in nitric acid, but under relatively weak oxidizing conditions, as in the vapor and condensate regions, exhibits a high corrosion rate [5, 6]. The corrosion resistance of titanium in condensed HNO_3 can be improved by alloying with refractory metals such as Tantalum (Ta) and

Niobium (Nb), which have same metallic ion size as of titanium, lowering its solubility in HNO_3 and forming a stable oxide film [7]. Addition of about 5 wt.% Ta to titanium almost doubles the corrosion resistance, while addition of up to 1.8 wt.% Nb to Ti–5 wt.% Ta enhances the corrosion resistance almost seven times. Hence, Ti–5%Ta–1.8%Nb alloy is found to be a potential candidate material for structural applications such as vessels for dissolvers and evaporators in nuclear fuel reprocessing plants [7, 8]. The physical metallurgy database for this alloy generated in our laboratory [9] based on X-ray diffraction and detailed transmission electron microscopy analysis classifies the alloy as two phase, containing (HCP) α and (BCC) β phases. β transus of the alloy was evaluated [9] to be 1,143 K. The mechanisms of transformation of the high temperature β, when subjected to isothermal or thermo-mechanical treatments in various phase fields have been studied in detail and the microstructural and microchemical characteristics of the resultant products have been established [9, 10]. A host of microstructures forms as the alloy transforms under different conditions of annealing temperature and cooling rate. The repartitioning of solutes Ta and Nb between the coexisting α and β phases introduces solute gradients within the matrix. This leads to differences in corrosion behavior among different microstructures. Hence, it is necessary to identify the alloy with a microstructure exhibiting superior corrosion resistance and design suitable treatments to achieve the optimum microstructure. The present paper reports the corrosion behavior of the alloy in different heat treatment conditions based on which the most suitable structure for the end application is identified.

Experimental

The Ti–5%Ta–1.8%Nb alloy was obtained from Nuclear Fuel Complex, Hyderabad in the form of an ingot of 150 mm and rods of 12.5 mm diameter. The former is the as cast alloy in ''β annealed'' condition while the latter is a product of ''thermo-mechanical processing'' [10]. The β annealed alloy was subjected to a series of thermal and mechanical processes for obtaining the 12.5 mm rods, which included hot extrusion in the two phase field (1,103–1,113 K), β quenching, tempering, cold swaging and intermittent stress relieving treatments in the range of 903–923 K. The chemical composition of the alloy is given in Table 1. The thermo-mechanically processed (TMP) alloy of 12.5 mm diameter was further cold rolled to sheet form (3 and 1.7 mm thick) and stress relieved at 913 K. This alloy is used as a reference and will be hereafter referred to as the ''reference alloy.'' These were subjected to a set of heat treatments in vacuum, such as Mill Annealing (MA), Solution Treatment (ST) followed by aging (STA) and over aging (STOA), the details of which are given in Table 2.

The specimens for optical and scanning electron microscopy were prepared by standard metallographic methods. Optical and scanning electron microscopies were carried out using a Leica MeF4A and Philips XL30 ESEM microscopes, respectively. Transmission Electron Microscopy on thin foils was carried out using a Philips CM200 with Energy Dispersive Spectrometer (Super Ultra Thin Window) and DX4 Analyser. The details of the experiments and analysis procedure are given elsewhere [9, 10].

The corrosion rates were measured in boiling nitric acid by standard practice similar to ASTM A262 practice C for AISI 304 L SS [11, 12]. The experimental set up used for the present study is shown in Fig. 1. Specimens of dimensions ~$10 \times 10 \times 2.5$ mm^3 were weighed up to an accuracy of 0.0001 g, before subjecting them to corrosion tests. The specimens were exposed for a total period of 240 h in 11.5 M boiling HNO_3 in liquid, vapor and condensate phases. The ratio of volume of solution to the total specimen surface area in liquid, vapor and condensate phases together was about 75 mL/cm^2. The design of the experimental set-up ensured that the corrosion rate of the sample in condensate phase is not influenced by dissolved ions, since the solution condensing in the inner vessel was automatically siphoned out and replenished at regular intervals. However, in the liquid zone, corrosion rate is influenced by dissolved ions and the concentrated soluble titanium ions in the solution act as inhibitors [5]. The change in weight and surface appearance were examined by removing the specimens after every 48 h. This test was repeated on three sets of samples to check the reproducibility of results. After completion of the test, corrosion rates in individual periods and average corrosion rate for five individual periods were calculated. The error in evaluation of corrosion rate arises due to measurement of surface area of small sized samples and small weight changes.

Results

This section presents the results of the study on influence of microstructural variations on the corrosion behavior. The

Table 1 Composition of the alloy

Element	Ta	Nb	Fe	O	N	C	H	Ti
Amount in wt.%	4.39	1.85	0.0263	501.5 ppm	47 ppm	125 ppm	9 ppm	Balance

Table 2 Details of heat treatments provided to the reference (cold rolled and stress relieved) Ti–5Ta–1.8Nb alloy

Heat treatment	Temperature (K)	Time (h)	Cooling method
Mill annealing	973	4	Air cooling
Solution treatment	1,113	2	Water quenching
Aging following solution treatment	823	4	Air cooling
Over aging following solution treatment	973	4	Air cooling

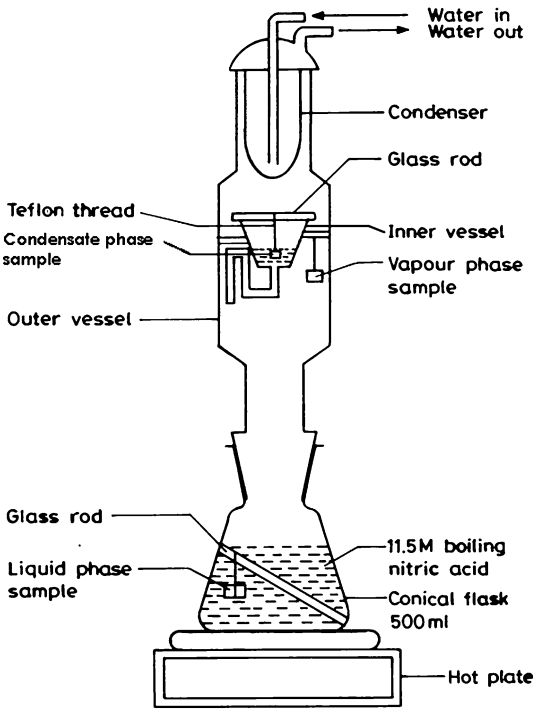

Fig. 1 Three phase corrosion test apparatus set up

results are organized as follows: Section ''Corrosion behavior of the ''as cast'' and reference alloy'' presents the corrosion behavior of the alloy in ''β annealed'' and reference conditions and the microstructural analysis. Section ''Optimization of microstructure through designed treatments for corrosion control'' presents the microstructural characterization of the alloy subjected to controlled heat treatments and the consequent corrosion behavior.

Corrosion behavior of the ''as cast'' and reference alloy

In the present study, general corrosion of the alloy is of concern. The corrosion rates of the as cast and reference alloys in the liquid, vapor and condensate phases are listed in Table 3. The corrosion rates of 304 Stainless Steel and CP titanium are also listed in Table 3 for comparison. It is very clear that Ti–5Ta–1.8Nb alloy exhibits superior corrosion resistance in comparison to 304L SS and commercially pure (CP) titanium, in all the three phases namely liquid, vapor and condensate. SS 304L exposed to 11.5 M nitric acid undergoes transpassive corrosion leading to a very high corrosion rate. However, the lower corrosion rate in the condensate phase in 6 M nitric acid is due to the passive nature of stainless steel. CP titanium has comparatively lower corrosion rates in liquid and vapor phase, but a high corrosion rate in the condensate phase. This is attributed to the unstable nature of the oxide layer that forms in the condensate phase. In fact, the main limitation of titanium has been its low corrosion resistance in the trickling acid condensate, which is due to the ''desquamation'' or in other words the destabilization of the oxide layer at the interface between liquid and vapor [13].

The corrosion rates measured in the as cast ''β annealed'' and reference alloys are 1.49 and 0.258 mpy, respectively, in the liquid phase. Such a large difference in the corrosion rates in the liquid phase clearly suggests that the alloy in the thermo-mechanically processed condition exhibits superior corrosion behavior. This suggests that the microstructure after thermo-mechanical processing which is expected to be significantly different from that of the β annealed alloy exerts a profound influence on the corrosion behavior. In order to understand the role of microstructure in governing the corrosion behavior a detailed microstructural characterization of the alloys was carried out.

Figure 2a, b shows the optical micrograph of the alloy in the as cast ''β annealed'' condition. Coarse grains with sizes as high as 2 mm are observed. Several colonies with uniform acicular structure are observed within the prior β grains. The average size of the colony was about 50 μm. Such a structure called ''transformed β structure'' in titanium alloys is reported to form by a Widmanstatten transformation during cooling of the high temperature β [14]. In addition to α colonies, the presence of α as a continuous film along the prior β grain boundaries is observed. This has been identified as the grain boundary α [15], which is the first phase to form due to availability of easy nucleation sites. The presence of such grain boundary α has been found to be deleterious causing embrittlement in similar titanium based alloys [16].

The Ti–5Ta–1.8Nb alloy has been classified as an $\alpha + \beta$ alloy in our earlier work [9], based on its chemistry and X-ray and electron diffraction evidences. Electron microscopy on thin foils of the β annealed sample carried out, to identify the nature of the fine acicular phases revealed a well resolved lamellar structure (Fig. 2c). Analysis of the Selected Area Diffraction (SAD) patterns taken from alternate lamellae (Fig. 2d, e) shows the presence of α phase along $[01\bar{1}1]$ and β phase along $[\bar{1}13]$ zone axis. This

Table 3 Comparison of three phase corrosion behavior of Ti–5Ta–1.8Nb alloy, CP Ti and SS 304 in 11.5 M HNO_3

Material/condition	Corrosion rate (mpy)		
	Liquid	Vapor	Condensate
Ti–5Ta–1.8Nb—β annealed	1.49	0.47	1.26
Ti–5Ta–1.8Nb—Reference	0.258	0.512	2.773
CP-Ti*	<0.39	1.38	15.75
304L SS*	177.00	11.81	3.54

* Reference [11]

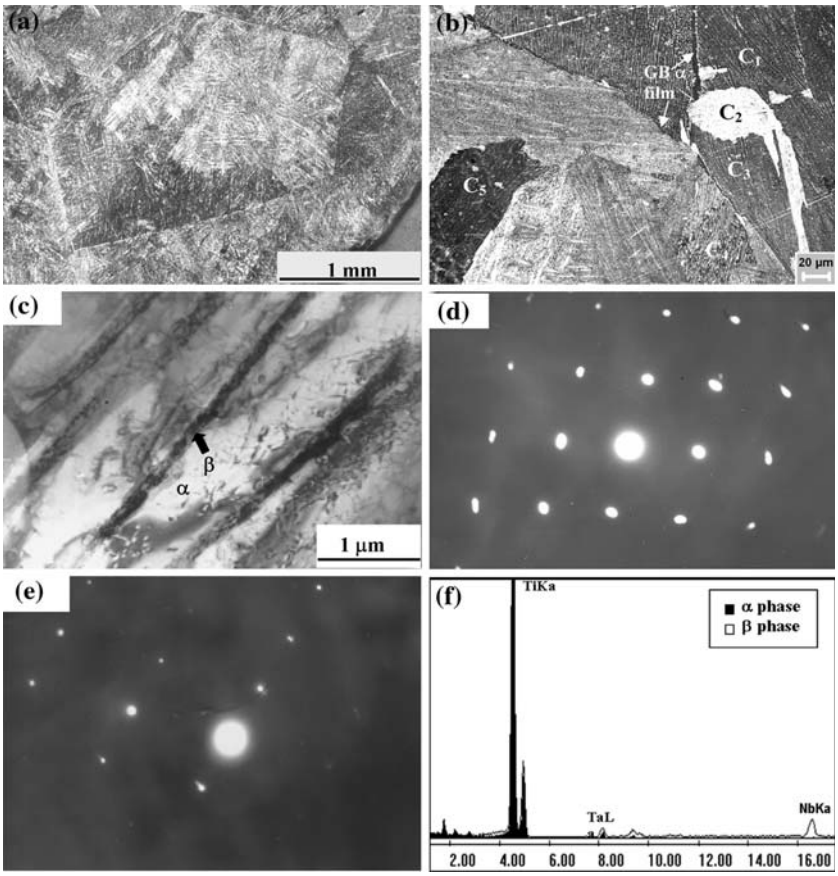

Fig. 2 Microstructure of the β annealed alloy showing (**a**) a full, coarse prior β grain, (**b**) GB α at the prior β grain boundaries and many α colonies within each prior β grain, (α colonies C_1, C_2, C_3 are within one β grain and C_4, C_5 are in another β grain) (**c**) alternate lamellae of α and β, (**d**, **e**) SAD taken from the α and β phases along the zone axes $[01\bar{1}1]$ and $[\bar{1}13]$, respectively, and (**e**) EDS spectra from α and β phases showing enrichment of the β phase with Ta and Nb

confirms that the microstructure termed as transformed β consists of alternate lamellae of α and β [14]. Widths of individual lamella were measured in the range of 0.1–1.06 μm and 0.01–0.25 μm, for α and β phases, respectively. About 12–15% of β phase was found be retained, which was estimated by conventional image analysis procedures.

It is well known that solute elements repartition between coexisting α and β phases depending on their propensity to stabilize α or β phase. Figure 2f shows the EDS spectra from α and β phases. An observable increase in the amount of Nb and Ta is clearly seen in β phase in comparison to α phase, confirming that there has been solute repartitioning. The above experiments showed that the as received ''β annealed'' alloy consists of a transformed β structure with alternate lamellae of solute lean α and solute rich β phases. This acicular structure with steep microchemical gradients between the constituents is expected [17] to lead to galvanic attack between the two phases enabling corrosion to penetrate along the needles. The higher corrosion rate measured for this specimen can probably be due to such a galvanic attack. Detailed analysis of the corroded samples is in progress to confirm this.

The existing industrial experience [17] with commercial grade titanium shows that failure of titanium equipment in nitric acid occurs due to preferential attack in weld regions. The failure is severe especially if the iron content is high, ≥0.05%. These failures have been understood as follows:

iron, whose solubility limit in α titanium is ~0.05%, is known to stabilize the high temperature bcc β phase and repartitions into the β phase when its concentration exceeds solubility limit. This introduces a solute gradient between adjacent phases. In the weld region, cooling the alloy from above β transus leads to formation of alternate lamellae of α and β—a microstructure most susceptible to corrosive attack. A similar effect has been observed in a number of titanium alloys used in corrosive media [18, 19]. From the above results, it can be inferred that the distribution of β phase in an acicular morphology is detrimental to corrosion resistance.

The lower corrosion rate measured in the reference alloy suggests that thermo-mechanical treatments had modified the morphology and distribution of the β phase. Hence, detailed microscopy analysis was carried out on the reference alloy. Figure 3a shows the microstructure of the reference alloy. A large volume fraction of equiaxed grains of sizes ranging from 12 to 15 μm is observed. Further, SEM observations (Fig. 3b) showed the presence of fine globular particles within the grains. These particles were observed to have sizes ranging from 100 to 500 nm and EDS spectra from these particles showed these are β phase particles.

Detailed transmission electron microscopy observation of this sample showed (Fig. 4) the presence of α in equiaxed and acicular morphologies, corresponding to the primary and secondary α phase. The precipitates were distributed as isolated globular particles, either along the grain boundaries of equiaxed primary α or along the boundaries of acicular α. The size of these particles ranged from 0.1 to 0.6 μm. Analysis of SAD pattern (inset in Fig. 4a) taken from an isolated particle along the grain boundary shows the presence of β along $[\bar{1}13]$ zone axis. The solute redistribution between primary α and globular β is shown in the EDS spectra in Fig. 4b. Higher amount of Ta and Nb in β is clearly observed, confirming the solute rich nature of the β phase. The above results show that the reference alloy consists of a microstructure with a large volume fraction of equiaxed α (~95%) and random distribution of discrete β particles. The low corrosion rate measured for this alloy suggests that a structure of polygonal α with a random distribution of isolated globular β particles is more desirable than alternate lamellae of α and β phases w.r.t corrosion behavior. Such an equiaxed structure in CP titanium [17] also has been reported to show lower corrosion rate compared to an acicular structure. The amount of α and β phases and their morphology is crucial in controlling corrosion rate. The change in corrosion behavior with microstructural variation is described in the next section.

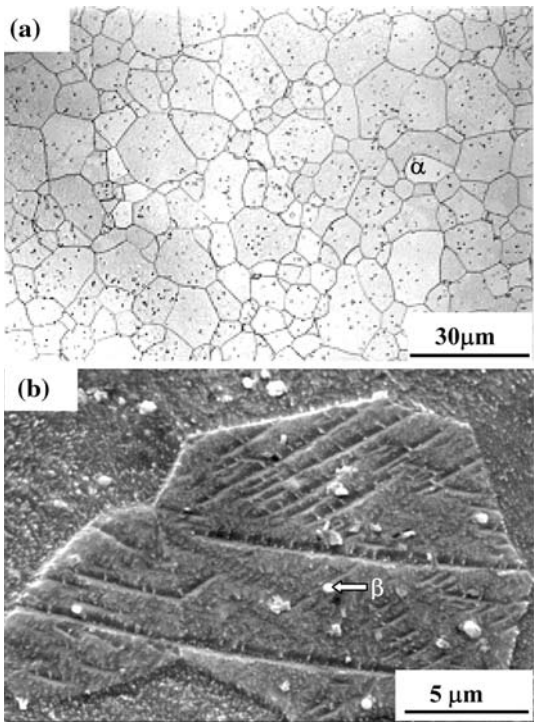

Fig. 3 Microstructure of the reference alloy showing (**a**) predominantly equiaxed structure in the optical micrograph and (**b**) fine intragranular β precipitates in the Secondary Electron image

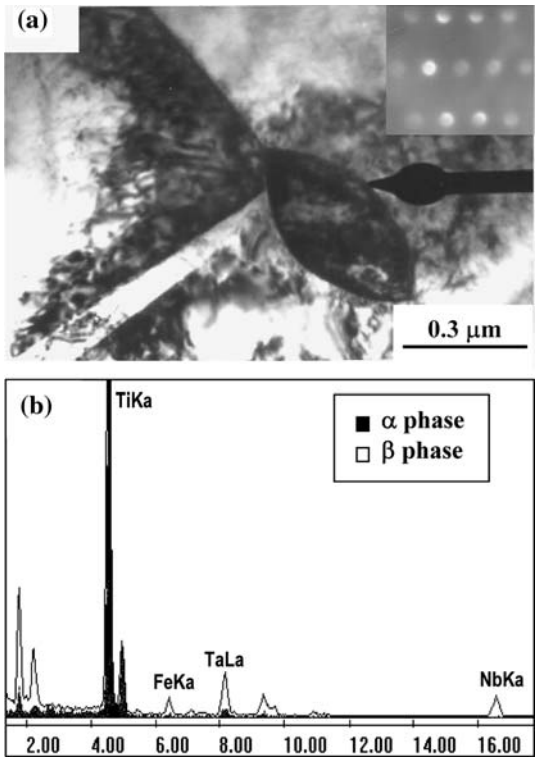

Fig. 4 (**a**) Transmission Electron micrograph of the reference alloy showing a β precipitate at the grain boundary triple point in an equiaxed α matrix; the inset shows the micro-diffraction pattern from the β phase along $[\bar{1}13]$ zone axis and (**b**) EDS spectra from α and β phases where the β phase is enriched with Ta, Nb and Fe

Optimization of microstructure through designed treatments for corrosion control

This section presents the results of the following systematic studies: (1) evolution of microstructure after subjecting to different heat treatments (Table 2) following the industrial experience of other α–β titanium alloys [20], (2) their corrosion behavior in the liquid, vapor and condensate phases of boiling nitric acid and (3) the surface morphology of the corroded surfaces.

Corrosion behavior of alloy subjected to designed heat treatments

The corrosion rates were measured in the three phases in boiling nitric acid for the alloy in mill annealed, solution treated, solution treated and aged/overaged conditions and the results are given in Table 4. The corrosion rates for all the treatments are low in the liquid and vapor phases, while the high corrosion rate in condensate phase suggests continuous dissolution. The typical corrosion rate for the heat-treated specimens is around 0–0.2 mpy in liquid phase, 0–0.7 mpy in vapor phase and 1.1–2.7 mpy in the condensate phase. The variation of corrosion rates in the three phases for different treatments is illustrated in Fig. 5.

The reference alloy shows average values of 0.26, 0.51, and 2.77 mpy in the liquid, vapor and condensate phases, respectively, which has been understood in terms of its microstructure. The mill-annealed sample showed similar corrosion rates.

Solution treatment of the reference alloy high in the $\alpha + \beta$ phase field resulted in lowering of corrosion rate in the liquid phase (0.258 and 0.061 mpy, respectively). However, the rates were higher than the reference structure in the vapor (0.512 and 0.736 mpy, respectively) and condensate (2.773 and 3.251 mpy, respectively) phases. Compared to the above structures (Table 4) the alloy in the aged condition showed the lowest corrosion rate in all the three phases. The overaged alloy showed corrosion behavior similar to that of the aged alloy.

The variation in corrosion behavior in the three phases is expected to arise from microstructural variations caused by the different treatments. Features that control the corrosion behavior could be the amount, size and morphology of α and β phases. Hence the microstructural modifications of the reference structure by the designed heat treatments are studied and results described in the next sub section.

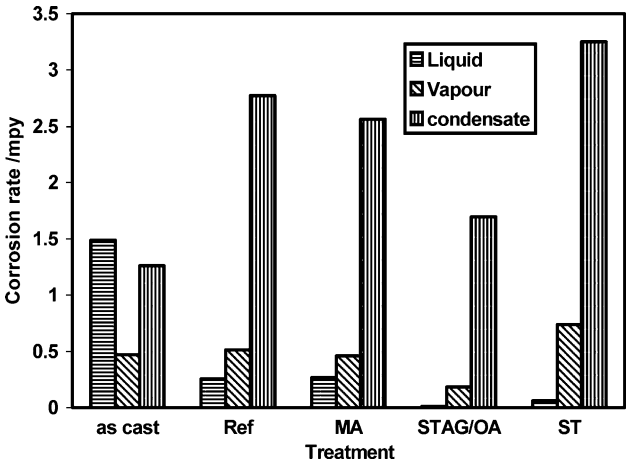

Fig. 5 Comparison of the three phase corrosion rates of the alloy subjected to different heat treatments

Modification of microstructures due to heat treatments to reference alloy

The microstructure of the alloy after the mill-annealing treatment in the $\alpha + \beta$ phase field is shown in Fig. 6a. The structure shows large volume fractions of equiaxed α with inter and intragranular precipitates of nodular β. The TEM micrograph in Fig. 6b shows the presence of intragranular β precipitates. The EDS spectra from the two phases in Fig. 6c show the clear enrichment of Ta and Nb in the β phase. Hence it is seen that the structure after mill-annealing treatment is similar to the reference alloy.

Solution treatment high in the $\alpha + \beta$ phase field followed by water quenching showed (Fig. 7a) a predominantly equiaxed α microstructure. But careful TEM observations showed the presence of intra and intergranular α' (Fig. 7b). Aging or over-aging of the solution treated alloy leads to the decomposition of the martensite into α and β phases, their amount dictated by the phase diagram. The microstructure of the alloy over-aged at 973 K is

Table 4 Average three phase corrosion rates of the Ti–5Ta–1.8Nb alloy subjected to different heat treatments

Treatment	Corrosion rate (mpy)		
	Liquid	Vapor	Condensate
Mill annealing	0.266	0.459	2.563
Solution treatment	0.061	0.736	3.251
Solution treatment + aging	0.0	0.183	1.697
Solution treatment + over aging	0.032	0.0	1.100

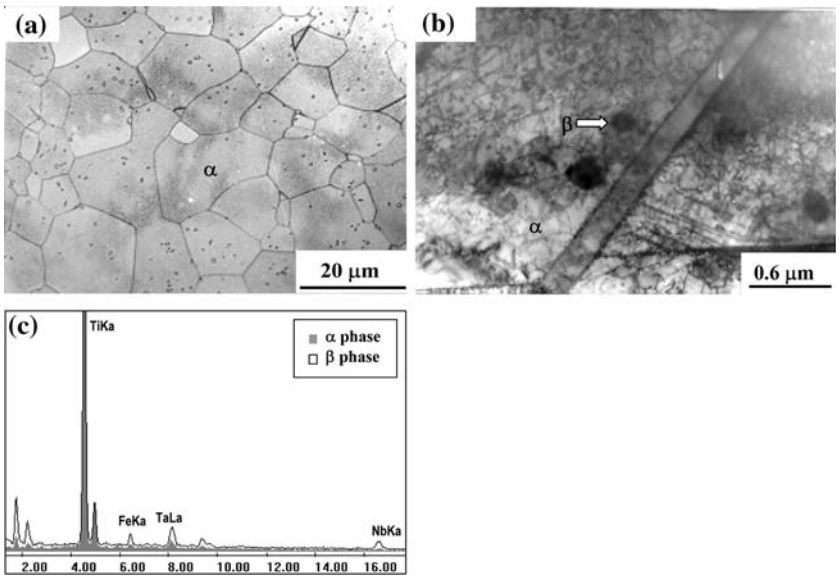

Fig. 6 Microstructure of the mill annealed alloy showing (**a**) equiaxed α (**b**) β precipitates in a α matrix and (**c**) EDS spectra from α and β phases showing enrichment of Ta, Nb and Fe in the β phase

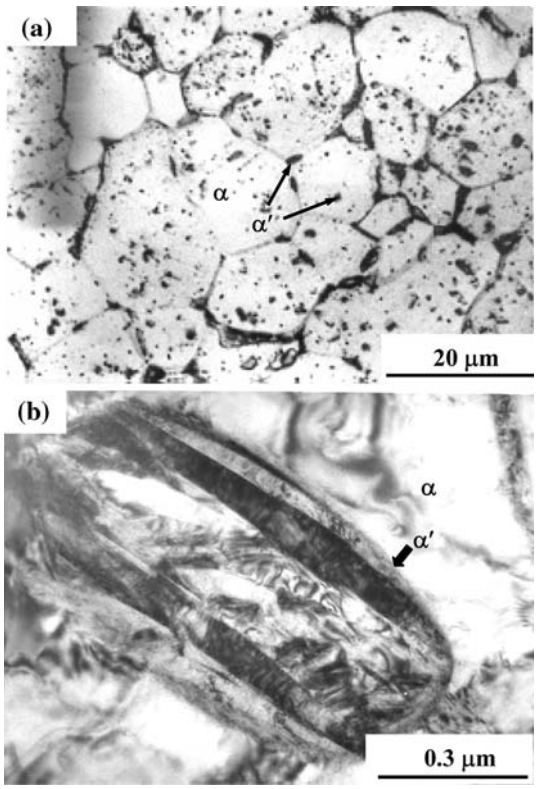

Fig. 7 Microstructure of the alloy solution treated at 1,113 K showing (**a**) formation of intra and intergranular β (α' on cooling) and (**b**) α' laths resolved at high magnification (arrow marked in (**a**))

shown in Fig. 8a. The presence of a large amount of equiaxed α is observed. The optical micrograph of the alloy aged at 823 K in Fig. 8b shows a microstructure similar to that of the overaged alloy. TEM micrograph of the alloy (Fig. 8c) after aging treatment shows fine β precipitates on the lath boundaries of martensite. EDS spectra from α and β phases in Fig. 8d shows the solute enrichment in β phase. Since the aging treatment has been carried out at a lower temperature, it is expected that the volume fraction of β phase to be lesser than that of the overaged alloy while the solute enrichment of β phase to be higher than the overaged alloy. Such a structure is considered beneficial with respect to corrosion resistance due to very low amount of β distributed as fine globular precipitates. This was evident from the lowest values of corrosion rates measured for this specimen. Hence the structure after solution treatment and aging can be summarized as a mixture of predominantly equiaxed α and tempered martensite.

The above results show that of the various treatments given to the Ti–5Ta–1.8Nb alloy, the alloy subjected to solution treatment and aging shows superior corrosion resistance. This treatment yields the most desirable microstructure of predominantly equiaxed α and minimum amount of fine, globular inter and intragranular β precipitates. The above studies have clearly elucidated the crucial role of microstructure in controlling the corrosion behavior in the Ti–5Ta–1.8Nb alloy.

Surface morphology of the alloy subjected to corrosion tests

The oxide film on titanium shows different colors on varying its thickness depending upon the nature of electrolyte and anodizing voltage due to interference effects. A visual examination of the oxides on samples exposed to the three phase corrosion test shows that the films are pale yellow to greenish in liquid phase, yellow in the vapor phase and gray in the condensate phase. It is reported that a yellow color indicates a film thickness of 100–250 Å, a

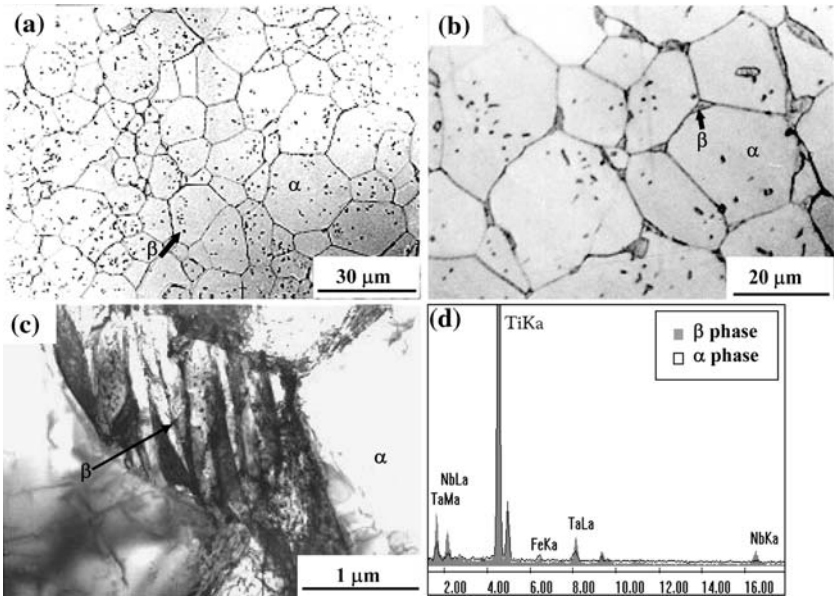

Fig. 8 Microstructure of the alloy showing intra and intergranular β after solution treatment followed by (**a**) overaging at 973 K and (**b**) aging at 823 K; (**c**, **d**) evidence for formation of fine β precipitates due to tempering of martensite formed during solution treatment in the alloy aged at 823 K. Enrichment of Ta and Nb in the β phase is clearly seen in (**d**)

bluish green color indicates a film thickness of 700–1,700 Å and above a thickness of 1,700 Å it is white [1]. The observation of similar colorations in the present study implies that the oxide film forming in the liquid phase is thicker as well as protective than the one formed in the vapor phase. This is because the rate of film formation increases when a certain amount of dissolved titanium ions in solution is reached by the corrosion process [21]. This was further confirmed from the Scanning electron micrograph of the mill annealed sample after corrosion tests in liquid, vapor and condensate phases shown in Fig. 9a–c. The surface morphology of the samples exposed to liquid and vapor phases does not show much change. This is also evident from the low corrosion rates in the liquid and vapor phases. But the sample exposed to condensate phase shows a thick, porous oxide layer. A similar behavior is also observed in the solution treated sample. A high corrosion rate in the condensate phase is attributed to the formation of a non-stoichiometric, non-protective oxide film, which is discussed in detail in Section ''Rationalization of the three phase corrosion behavior.'' In contrast, the overaged alloy showed a different surface morphology (Fig. 10a, b). The underlying microstructure is revealed suggesting very little dissolution of the surface film as is also evident from the low corrosion rates in condensate phase.

Discussion

The first part of the discussion briefly highlights the possible phase transformations during the various heat treatments. Later the corrosion behavior is discussed in detail. It is known that the metal oxides are largely ionic compounds, with metal and oxide ions in their respective crystal lattices. Titanium is known to form n-type or negative carrier type oxide namely TiO_2, in which there is an excess of metal ions at interstitial positions or anion (O^{2-}) vacancies [22]. This can be attributed to the presence of Ti^{3+} ions to maintain electrical neutrality, making the TiO_2 film non-stoichiometric. It has also been shown that in the case of zirconium and titanium, the oxide ions diffuse inwards to react at the metal/oxide interface. Thus, the growth of n-type oxide film is through the simultaneous diffusion of positive titanium ions and negative O^{2-} ions in opposite directions. The above theory, well established for high temperature oxidation is also reported to be valid for aqueous corrosion in Ti alloys [6]. The corrosion of metal in aqueous media results in the formation of oxide film on the surface of the metal by the following chemical reactions in the liquid and condensate phase.

$$\text{Liquid phase : } Ti \rightarrow Ti^{3+} + e^-$$
$$Ti^{3+} \rightarrow Ti^{4+} + e^-$$
$$Ti^{4+} + 2H_2O \rightarrow TiO_2 + 4H^+$$

$$\text{Condensate phase : } Ti \rightarrow Ti^{3+} + e^-$$
$$2Ti^{3+} + 3H_2O \rightarrow Ti_2O_3 + 6H^-$$

When titanium is alloyed with pentavalent elements like Ta or Nb, there is an annihilation of anion vacancies. Nb^{5+} or Ta^{5+} ions increase the concentration of anions and make the oxide film less defective. Thus, the oxide film becomes more stable and passive [23]. Ti–5%Ta–1.8%Nb alloy is expected to form Ta and Nb rich stable TiO_2 films as these elements are less soluble in nitric acid, which acts as a

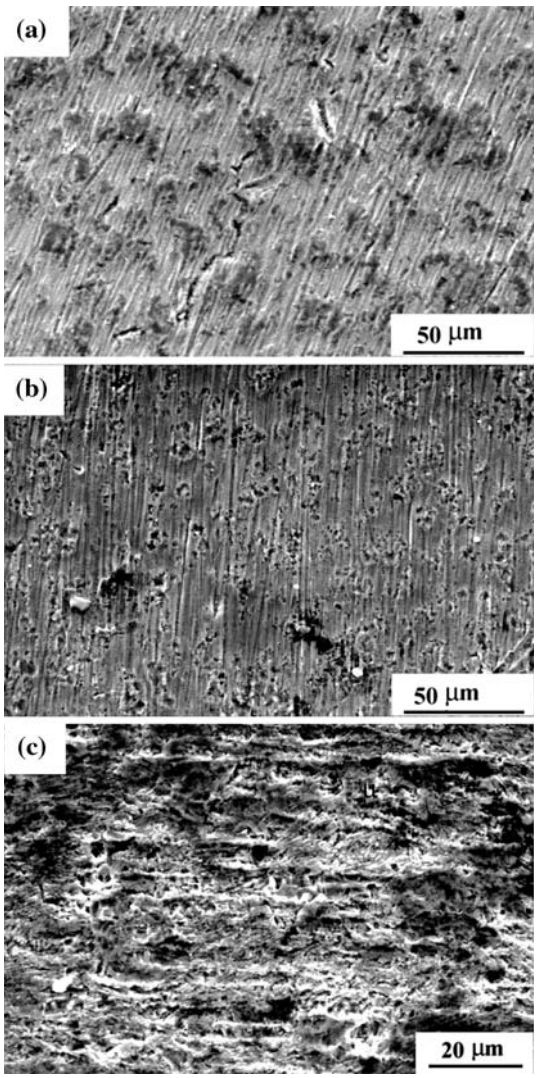

Fig. 9 SEM micrograph of the corroded surface of the mill annealed alloy after subjected to three phase corrosion test, showing (**a**, **b**) low corrosion in the liquid and vapor phases and (**c**) an accelerated attack in the condensate phase

barrier for further corrosion to take place. The mechanism of corrosion in the three phases and the role of microstructure in altering the corrosion resistance are discussed in the following subsections.

Phase transformation mechanisms in the reference alloy during the designed heat treatments

The evolution of reference structure of equiaxed α and fine β precipitates from an β annealed structure of alternate lamellae of α and β phases during the different stages of thermo-mechanical processing has been discussed in detail in earlier studies [10]. In the present study microstructural evolution during the different heat treatments can be understood as follows: the mill annealing treatment has not resulted in any major change of microstructure but only a

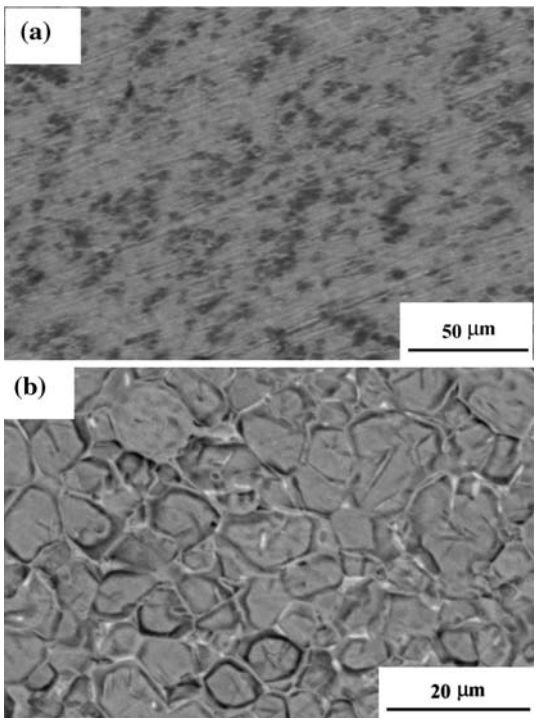

Fig. 10 SEM micrograph of oxide layers in the solution treated and overaged alloy subjected to three phase corrosion test, showing negligible change in the surface morphology in (**a**) liquid and (**b**) condensate phases

slight increase in the amount of β with a concomitant decrease in the solute content. The solution treatment has been carried out at a temperature higher than the Ms temperature [9] of the alloy and hence the β phase formed at the solution treatment temperature undergoes a martensitic transformation on quenching. It is reported [24] that in the case of eutectoid systems, hcp α' decomposes into α phase and non-coherent intermetallic compound through several stages, but in the case of isomorphous systems, α' decomposes into equilibrium α and β phases directly, where the β phase heterogeneously nucleates at the lath boundaries and internal substructures. The composition of α' approaches that of α, in equilibrium with β, depending on the temperature and duration of the treatment. Hence, the precipitation of β phase as fine, isolated, globular particles during the aging and overaging treatments is due to tempering of α' in the solution treated alloy. Hence the amount of β phase should be higher in the case of overaged sample than the aged sample, but the solute enrichment of the β phase would follow an inverse relation in these two cases.

Rationalization of the three phase corrosion behavior

The corrosion resistance of titanium alloys is generally high in oxidizing acids like nitric acid over the complete

concentration range at sub-boiling temperatures. But its corrosion resistance above 80 °C is highly dependent on the purity of nitric acid [25]. It has been reported that mid-range HNO_3 concentrations (20–70%) are most aggressive when full inhibition to attack is not achieved in pure refreshed solutions [17, 25]. As the impurity levels increase in hot HNO_3 solutions, the corrosion resistance of titanium improves significantly. Relatively small amounts of certain dissolved metallic ions like Si^{4+}, Fe^{3+}, Cr^{6+}, Ti^{4+} [25] can effectively inhibit the high temperature corrosion of titanium in nitric acid. This self-inhibition effect due to dissolved Ti^{4+} ions accounts for the lowest corrosion rate in the liquid phase for all treatments. Though, β stabilizers in general reduce the corrosion resistance of titanium, addition of Ta and Nb, which themselves have a high resistance to nitric acid, is beneficial, since they reduce the minimum amount of dissolved Ti^{4+} ions required to form a stable oxide.

The corrosion resistance of the alloy is also strongly dependent on the nature of oxide film that forms on the surface. Based on thermodynamic calculations, it is reported [26] that the anodic oxide film formed on transition metals like titanium consists of two layers, the lower oxide Ti_2O_3 at the metal oxide interface and the higher oxide TiO_2 at the oxide electrolyte interface. The corrosion rate is therefore determined by the combined effect of the above factors.

The corrosion rate of the alloy in the liquid phase (Table 4) is minimum for all the treatments. The minimum titanium ion content that leads to passivation depends on the acid concentration. Titanium shows maximum corrosion in 40–50% boiling nitric acid if renewed periodically and minimum corrosion if the solution is not renewed. This implies that the amount of dissolved titanium ions in liquid phase in this concentration range is high enough giving rise to a thicker protective oxide film.

It is seen from Table 4 that the corrosion rate in the vapor phase is slightly higher than that in the liquid phase. This shows that the conditions prevailing in the vapor phase is different from that in the boiling liquid. The nitric acid vapors, which have the same temperature as the boiling nitric acid but a lower concentration (6 M), are weakly oxidizing. This could result in the formation of a thin layer of semi-protective Ti_2O_3 instead of the fully protective TiO_2 film, which could be responsible for the higher corrosion rate in the vapor phase compared to the liquid phase.

The alloy shows the highest corrosion rate in the condensate phase. The condensate phase like the vapor phase is very weakly oxidizing and a non-stoichiometric Ti_2O_3 film forms. Additionally due to the continuous renewal of the solution, the concentration of dissolved Ti^{4+} ions in this region is negligible [5, 27]. Under flowing conditions, this oxide film does not adequately retard continued oxidation of the metal surface. Hence, the formation of a non-stoichiometric, unstable oxide film and absence of accumulation of inhibiting titanium ions are the main factors responsible for the high corrosion rate in the condensate phase for all treatments.

Effect of microstructure on corrosion rate in different phases of nitric acid

Though in general single-phase titanium alloys are most resistant to corrosion, it is reported that $\alpha + \beta$ alloys provide a good combination of corrosion resistance and mechanical properties [28, 29]. Yu and Scully [30] observe that β solution treated Ti–15Mo–3Nb–3Al exhibits a better corrosion resistance as compared to the aged microstructure, due to repartitioning of the alloying elements during aging process. But Thair [31] reports that Ti–6Al–7Nb with a dual microstructure of α and β phases exhibit better corrosion resistance than β heat treated samples. These results suggest that corrosion behavior is influenced by the characteristics of the oxide film, which in turn is dependent on the microstructure.

It is reported that when alloying elements form an oxide, they occur as discrete clusters embedded in a titanium matrix [32]. Therefore the uniform distribution of fine β particles that are enriched with Ta and Nb can be expected to form a stable passive layer, which would result in a better corrosion resistance. The superior corrosion resistance observed in the aged and overaged microstructures is therefore attributed to the presence of such fine β precipitates distributed on the lath boundaries and dislocations, while the mill annealed and reference structures with a distribution of coarse β precipitates exhibit a lower corrosion resistance in all the three phases as discussed in Section ''Optimization of microstructure through designed treatments for corrosion control.'' Sittig et al. [33] report that in the dual phase alloy Ti–6Al–7Nb, the α phase dissolves in preference to the Nb enriched β phase in a pickling medium of $HF + HNO_3$, since the local composition of oxide layer follows that of the underlying microstructure. Although a non-stoichiometric Ti_2O_3 oxide film forms in flowing conditions, the presence of retained β precipitates enriched with Ta and Nb stabilizes the oxide film in the condensate and vapor phases, where the accumulation of Ti^{4+} ions is negligible. This behavior can be understood by referring to the pseudo binary diagram of β isomorphous Ti alloys. At low temperatures, the amount of β phase is low with a concomitant increase in the amount of β stabilizers. The amount of α phase and solubility of β stabilizers like Ta and Nb in the α phase can be increased by carrying out treatments low in the $\alpha + \beta$ phase field, as in the case of solution treated and aged or overaged

Table 5 Effect of microstructural features on the three phase corrosion behavior

Treatment	Corrosion rate in comparison to the reference alloy	Microstructure	Effect of microstructure	Cause
β annealing	Higher	Lamellar $\alpha + \beta$	Detrimental	Detrimental due to formation of micro-galvanic cells between the α and β phases
Reference	0.258–2.77 mpy	Equiaxed α + coarse nodular β	Desirable	Random distribution of β precipitates in equiaxed α reduces tendency for formation of micro-galvanic cells
Mill annealing	Comparable	Equiaxed α + coarse nodular β	Desirable	Reasons similar to that for reference alloy
Solution treatment	Lower in liquid phase and higher in vapor and condensate phases	Equiaxed α + martensite	Detrimental	Oxide film in absence of β is less protective in all three phases, but is compensated by the inhibiting effect of dissolved titanium ions in the liquid phase
Solution treatment + aging	Lower	Equiaxed α + fine nodular β	Most desirable	Increased stability of oxide film and hence lower dissolution rate due to uniform distribution of fine β particles
Solution treatment + over aging				

microstructures. The α phase is therefore not fully depleted of Ta and Nb, but is lean compared to that of β precipitates. Hence, the oxide film over α phase also incorporates Ta and Nb in its lattice making it nearly stoichiometric and hence protective [23]. This explains the role of low amounts of β phase in reducing the corrosion rates in the solution treated and aged or overaged microstructure.

It was reported in Section ''Optimization of microstructure through designed treatments for corrosion control,'' that the solution treated alloy shows a high corrosion rate in the vapor and condensate phases. This can be understood from the microstructure, which consists of a large volume fraction of α' with low enrichment of β stabilizers distributed inhomogeneously. In the absence of highly enriched β precipitates, the oxide film is not expected to be as protective as in the other two cases. This explains for the higher corrosion rate exhibited by the solution treated alloy in the vapor and condensate phases. On the other hand, in the liquid phase the solution treated alloy exhibits a lower corrosion rate than the reference structure. This is due to the inhibiting effect of the dissolved titanium ions, which compensates for the non-protective nature of the oxide film. The effect of microstructural variations on corrosion rate of Ti–5%Ta–1.8%Nb alloy in the three phases is consolidated in Table 5.

The following additional observations were made from the corrosion behavior of the Ti–5%Ta–1.8%Nb alloy.

- The aged and overaged alloys showed the same corrosion behavior in all the three phases, though a study of their microstructure shows that they contain different amount of retained β phase. Similarly, the reference and mill annealed alloys showed same corrosion behavior, although their β content is different.
- The mill annealed and overaged alloys showed very different corrosion behavior, though the amount of β phase is same.

The observations in the present study regarding corrosion behavior of Ti–5Ta–1.8Nb alloy with different microstructures are understood in the light of the above discussion. The alloy given different heat treatments can be sequenced in the increasing order of corrosion rate as follows: solution treated and aged, solution treated and overaged, solution treated, mill annealed and the reference. There are three microstructural features which directly play a crucial role in determining the corrosion rate: (1) a microstructure with fine β particles in an equiaxed α matrix results in a stable oxide film as compared to coarse β particles, (2) presence of Nb and Ta in the α and β phases enhances the stability of the oxide film and, (3) presence of Nb and Ta in α phase as a consequence of low amount of β phase reduces the amount of dissolved titanium ions which act as inhibitors.

Conclusions

The influence of microstructure on the three phase corrosion behavior in boiling nitric acid has been studied in a

Ti–5%Ta–1.8%Nb alloy and the role of microstructural features has been understood. The important results of the study are as follows.

- An equiaxed α structure with random distribution of β particles exhibits a better corrosion resistance in all the three phases in comparison to an alloy with a lamellar α–β structure.
- The liquid phase shows minimum corrosion rate while the condensate phase shows the highest corrosion rate for all microstructures.
- Of the different microstructures obtained by various treatments such as mill annealing, solution treatment followed by aging or over aging, the alloy in solution treated and aged condition exhibited superior corrosion resistance.
- The solution treated and aged alloy consisted of a microstructure of equiaxed α and a tempered martensite with fine β precipitates on lath boundaries and dislocations. Such a microstructure with fine, solute enriched β precipitates forms a protective oxide film, which is more stable as compared to the film that forms on microstructures either with coarse β precipitates or α'.
- The corrosion behavior of the Ti–5%Ta–1.8%Nb alloy in the three phases has been understood in terms of the combined effects of the stability of the protective oxide film that forms on the surface and the inhibiting effect of dissolved titanium ions in the solution.
- Crucial microstructural parameters that affect the corrosion rate are size, distribution and enrichment of β phase in an equiaxed α matrix.

Acknowledgements The authors wish to acknowledge Dr Baldev Raj, Director, IGCAR, Kalpakkam for his encouragement and keen interest in their pursuit on studies in titanium alloys.

References

1. Kamachi Mudali U, Dayal RK, Gnanamoorthy JB (1993) J Nucl Mater 203:73
2. Furuya T, Satoh H, Shimogori K, Nakamura Y, Matsumoto K, Komori Y, Takeda S (1984) In: Proceedings of ANS topical meeting, vol I, p 1.249
3. Kiuchi K, Hayashi M, Hayakawa H, Sakairi M, Kikuchi M (1994) ''Fundamental study of controlling factors on reliability of fuel reprocessing plant materials used in nitric acid solutions'', a poster paper in session: ''Corrosion and materials selection''. In: Proceedings of the fourth international conference on nuclear fuel reprocessing and waste management, RECOD '94, vol III, London, 24–28 April 1994
4. Ronald WS (1995) In: Baboian R (ed) Corrosion tests and standards: application and interpretation. ASTM manual series: MNL 20. ASTM, Philadelphia, USA, p 493
5. Steele DF (1986) Atom. March:5
6. Furuya T, Kawafuku J, Satoh H, Shimogori K, Aoshima A, Takeda S (1991) ISIJ Int 31(2):189
7. Kiuchi K, Hayakawa H, Takagi Y, Kikuchi M (1994) ''New alloy development for fuel reprocessing plant materials used in nitric acid solutions'', a poster paper in session: ''Corrosion and materials selection''. In: Proceedings of the fourth international conference on nuclear fuel reprocessing and waste management, RECOD '94, vol III, London, 24–28 April 1994
8. Kapoor K, Kain V, Gopal Krishna T, Sanyal T, De PK (2003) J Nucl Mater 322:36
9. Mythili R, Thomas Paul V, Saroja S, Vijayalakshmi M, Raghunathan VS (2005) Mater Sci Eng A390:299
10. Mythili R, Saroja S, Vijayalakshmi M, Raghunathan VS (2005) J Nucl Mater 345:167
11. Ravishankar A, Mythili R, Raju VR, Saroja S, Dayal RK, Vijayalakshmi M, Raghunathan VS, Balasubramaniam R, Singhal LK (2003) In: Raj B, Bhanu Sankara Rao K, Shankar P, Murali N (eds) Proceedings of conference on materials and technologies for nuclear fuel cycle, Chennai, India, 15–16 December 2003, p C-7
12. Ravi Shankar A (2004) Corrosion behaviour of Ti-5%Ta-1.8%Nb alloy in nitric acid medium for fast reactor fuel reprocessing applications. M. Tech. Thesis, Indian Institute of Technology, Kanpur, India
13. Bernard C, Mouroux JP (1991) In: Proceedings of the third international conference on nuclear fuel reprocessing and waste management, RECOD '91, vol II, Sendai, Japan, 14–18 April 1991, p 570
14. Flower HM (1990) Mater Sci Tech 6:1082
15. Gill FJ, Genebra MP, Manero JM, Planell JA (2001) J Alloys Compd 329:142
16. Zhang XD, Bonniwell P, Fraser HL, Baeslack WA III, Evans DJ, Ginter T, Bayha T, Cornell B (2003) Mater Sci Eng A343:210
17. Publication of Imperial Metal Industries (1969) Corrosion characteristics of titanium in ''Corrosion resistance of titanium'', Witton, UK, p 39
18. Brossia CS, Cragnolino GA (2001) Corrosion 57(9):768
19. Dull L, Raymond L (1969) J Electrochem Soc 116:332
20. Lampman S (1987) In: Steven RL, Scott DH (eds) ASM Metals Hand book, vol 2, ''Properties & Selection: Non-ferrous Alloys & Special Purpose Materials'', 10th edn. ASM International, Materials Park, OH, USA, p 592
21. Robin A, Sandim HRZ, Rosa JL (1999) Corr Sci 41:1333
22. Kenneth RT, Chamberlain J (1988) Corrosion for students of science and engineering. John Wiley and Sons Inc., USA, p 335
23. Metikos-Hukovic M, Kwokal A (2003) J Piljac, Biomater 24:3765
24. Williams JC (1973) In: Jaffee RI, Burte HM (eds) Titanium science and technology, vol 3, Plenum Press, New York, p 1433
25. Ronald WS, David ET (1987) In: Joseph RD, James DD (eds) ASM Metals Handbook, vol 13, ''Corrosion'', 9th edn. ASM International, Materials Park, OH, USA, p 669
26. Pergament AL, Stefanovich GB (1998) Thin Solid Films 322:33
27. Te-Lin Y (1986) In: Young CS, Durham JC (eds) Industrial applications of titanium, zirconium: vol 4, ASTM STP 917. ASTM, Philadelphia, p 57
28. Bomberger HB (1984) In: Webster RT, Young CS (eds) Industrial applications of titanium and zirconium: third conference, STP 830. ASTM, Philadelphia, p 143
29. Khan MA, Williams RL, Williams DF (1996) Biomaterials 17(22):2117
30. Yu SY, Scully JR (1997) Corrosion 53(12):965
31. Thair L (2002) Studies on thermomechanically processed and nitrogen ion implanted Ti-6Al-7Nb biomedical alloy. PhD Thesis, Anna University, Chennai, India
32. Marc Long HJ, Rack H (1998) Biomaterials 19:1621
33. Sittig C, Textor M, Spencer ND, Wiland M, Vallotton PH (1999) J Mater Sci: Mater Med 10:35